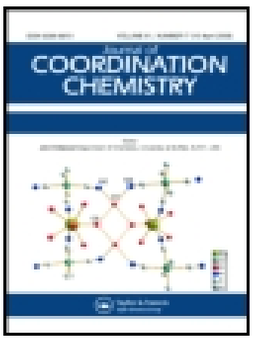

Journal of Coordination Chemistry

ISSN: 0095-8972 (Print) 1029-0389 (Online) Journal homepage: http://www.tandfonline.com/loi/gcoo20

Cobalt(II) complexes with pyridine and 5-[(*E*)-2-(aryl)-1-diazenyl]-quinolin-8-olates: Synthesis, electrochemistry and X-ray structural characterization

Tushar S. Basu Baul, Khrawborlang Nongsiej, Bruno G. M. Rocha & M. Fátima C. Guedes da Silva

To cite this article: Tushar S. Basu Baul, Khrawborlang Nongsiej, Bruno G. M. Rocha & M. Fátima C. Guedes da Silva (2018): Cobalt(II) complexes with pyridine and 5-[(*E*)-2-(aryl)-1-diazenyl]-quinolin-8-olates: Synthesis, electrochemistry and X-ray structural characterization, Journal of Coordination Chemistry, DOI: 10.1080/00958972.2018.1506876

To link to this article: https://doi.org/10.1080/00958972.2018.1506876

Cobalt(II) complexes with pyridine and 5-[(*E*)-2-(aryl)-1-diazenyl]-quinolin-8-olates: Synthesis, electrochemistry and X-ray structural characterization

TUSHAR S. BASU BAUL*†, KHRAWBORLANG NONGSIEJ†, BRUNO G. M. ROCHA‡ and M. FÁTIMA C. GUEDES DA SILVA*‡

†Centre for Advanced Studies in Chemistry, North-Eastern Hill University, NEHU Permanent Campus, Umshing, Shillong 793022, India
‡Centro de Química Estrutural, Complexo I, Instituto Superior Técnico, Universidade de Lisboa, Av. Rovisco Pais, 1049-001 Lisboa, Portugal

Nine new cobalt(II) compounds, *trans*-[Co(L^{PAQ})$_2$(Py)$_2$] (**1**), *trans*-[Co(L^{PAQ})$_2$(3-MePy)$_2$] (**2**), *trans*-[Co(L^{MeAQ})$_2$(Py)$_2$] (**3**), *trans*-[Co(L^{OMeAQ})$_2$(Py)$_2$] (**4**), *trans*-[Co(L^{OEtAQ})$_2$(Py)$_2$]·2(H_2O) (**5**), *trans*-[Co(L^{CAQ})$_2$(Py)$_2$] (**6**), *trans*-[Co(L^{BAQ})$_2$(Py)$_2$] (**7**), *cis*-[Co(L^{BAQ})$_2$(3-MePy)$_2$] (**8a**) and *trans*-[Co(L^{BAQ})$_2$(3-MePy)$_2$]·2(3-MePy) (**8b**) (primary ligand: L^{XAQ} = substituted 5-[(*E*)-2-(aryl)-1-diazenyl]quinolin-8-olate; secondary ligands: Py = pyridine, 3-MePy = 3-methylpyridine), have been synthesized and characterized by elemental analysis, IR and UV-vis spectroscopy. Magnetic measurements of the cobalt compounds were performed in solution by ^{1}H NMR spectroscopy using the Evans' method while their redox properties were studied by cyclic voltammetry. Single-crystal X-ray diffraction analysis of the compounds revealed their octahedral geometries and *trans* configuration, except for **8a**, which has a *cis* configuration. Intermolecular non-covalent interactions were detected, π···π interactions in **5**, C–H···π interactions in **2** and C–H···π edge-to-face (T-shaped) arrangements in **3**, **4**, **6** and **7**.

Keywords: Substituted quinolin-8-olate; Cobalt; Secondary ligands; Magnetic moment; Electrochemistry; Structure elucidation

1. Introduction

Quinolin-8-ol (HL^Q) is a well-known complexone or sequestering reagent, which possesses two potential protonation sites, a pyridyl nitrogen atom and a phenolate oxygen atom [1, 2]. A structural perspective of HL^Q in medicinal chemistry pertaining to biological activities, interactions with metal ions and mechanisms of action has been described [3]. The ligand L^Q

*Corresponding authors. Email: basubaul@nehu.ac.in, basubaulchem@gmail.com (T.S. Basu Baul); fatima.guedes@tecnico.ulisboa.pt (M. Fátima C. Guedes da Silva)

chelates most of the di-valent ([$M(L^Q)_2$], M = Mn, Co, Ni, Cu and Zn) and tri-valent metal ions ([$Al(L^Q)_3$]), and consequently can be used in an arsenal for various applications in supramolecular sensors, emitting devices or self-assembled aggregates [4-12]. Research efforts have also focused on thin film formation of nano-sized metal quinolin-8-olates (*e.g.* ([$M(L^Q)_2$], M = Co, Ni, Cu and Zn and ([$Fe(L^Q)_3$]) by application of the layer-by-layer deposition technique [13]. [$Co(L^Q)_2$] and [$Ni(L^Q)_2$]·$2H_2O$ complexes with 1D nanobelt structures were obtained via low-heating solid-state chemical reactions [14]. An example of a tetranuclear cluster with a [$Co_4(L^{OQ})_6Cl_2$] composition is also reported where the complex has four cobalt ions in two different coordination environments, two of them with chloride ligands. Chelated L^{OQ} (OQ = oxyquinolin-8-olate) ligands on cobalt ions also serve as bridging ligands by connecting the metals through μ-oxo-bridges [15]. The HL^Q scaffold has been functionalized by electrophilic aromatic substitution at the 5-position to obtain 5-[(E)-2-(aryl)-1-diazenyl]-quinolin-8-ol (HL^{XAQ}), which is long known as an analytical reagent for qualitative detection of metal ions [16]. The coordinating behaviors of such reagents were then investigated towards transition metals [17], Hg [18], U [19], R_nSn [20], mixed organotin-transition metals [17], mixed ligand organotin complexes [21] and rare earth compounds [22]. Further, considerable efforts have been made to design and to optimize the chemical properties of transition metal HL^{XAQ} complexes towards new colorimetric sensors [23], porous fumed silica covalently grafted with HL^{XAQ} to be used as extractants for Cu(II) and Ni(II) at low concentration levels [24] and nanosized [$Co(L^{XAQ})_2$] thin films using a new exciting, static, step-by-step soft surface reaction (SS-b-SSR) technique to achieve biological and optical properties [25].

Cobalt has become an ideal candidate to prepare metal complexes due to its diverse coordination geometries, large magnetic anisotropy and high Curie temperature [26]. The affinity of HL^Q for cobalt(II) falls within the classical order of stability $Mn^{2+} < Co^{2+} < Ni^{2+} < Cu^{2+} > Zn^{2+}$ and the same stability sequence is also observed for other HL^Q derivatives [27]. Although cobalt complexes with HL^{XAQ} of composition [$Co(L^{XAQ})_2$] are known, to our knowledge structurally characterized [$Co(L^Q)_2$] and [$Co(L^{XAQ})_2$] complexes have not been described yet, probably owing to their amorphous nature. The applicability of single crystals is evident in various fields such as semiconductors, polarizers, infrared detectors, solid state lasers, non-linear optics, piezoelectric, acoustic-optics, photosensitive materials and crystalline thin films for microelectronics and computer industries, *etc.* [28]. In view of these, attention has now been

diverted to the synthesis of new Co(II) complexes based on HL^{XAQ}, and the choice of the complexing agent rests upon the following criteria: (i) azo compounds based on HL^{Q} derivatives play a central role as chelating agents and their synthetic versatility allows the generation of a large number of derivatives; (ii) the incorporation of pyridine-based ancillary ligands in reactions with Co(II) may enhance the solubility of the amorphous $Co(L^{XAQ})_2$ compounds in addition to their inclusion in the coordination sphere of the metal, therefore providing a basis for the formation of stable novel mixed-ligand complexes of diverse dimensionalities and enabling their structural determination; (iii) the resulting compounds may exhibit intense optical absorptions over the visible region that lead to dye properties in coordination complexes; and (iv) to study the influence of the substituents of 5-[(*E*)-2-(aryl)-1-diazenyl]quinolin-8-olate on the redox properties of the compounds.

In a previous work [29], we investigated the intriguing influence of pyridine derivatives on the synthesis of a range of Zn(II) compounds with N,O-chelating HL^{XAQ} ligands. However, the design and synthesis of Co(II) coordination compounds with HL^{XAQ} ligands with predictable aggregate and topology remains a challenging task. In this context, a series of nine new compounds, *trans*-$[Co(L^{PAQ})_2(Py)_2]$ (**1**), *trans*-$[Co(L^{PAQ})_2(3\text{-MePy})_2]$ (**2**), *trans*-$[Co(L^{MeAQ})_2(Py)_2]$ (**3**), *trans*-$[Co(L^{OMeAQ})_2(Py)_2]$ (**4**), *trans*-$[Co(L^{OEtAQ})_2(Py)_2]\cdot 2(H_2O)$ (**5**), *trans*-$[Co(L^{CAQ})_2(Py)_2]$ (**6**), *trans*-$[Co(L^{BAQ})_2(Py)_2]$ (**7**), *cis*-$[Co(L^{BAQ})_2(3\text{-MePy})_2]$ (**8a**) and *trans*-$[Co(L^{BAQ})_2(3\text{-MePy})_2]\cdot 2(3\text{-MePy})$ (**8b**), scheme 1, were synthesized. The Co(II) compounds were structurally characterized by IR and UV-Vis spectroscopy and by single-crystal X-ray diffraction analysis. It is anticipated that the different pyridine ligands used in the cobalt compounds may influence the molecular and supramolecular structures, which ultimately modify the electronic features for future solid-state applications. The magnetic and redox properties of **1**-**8** were also studied.

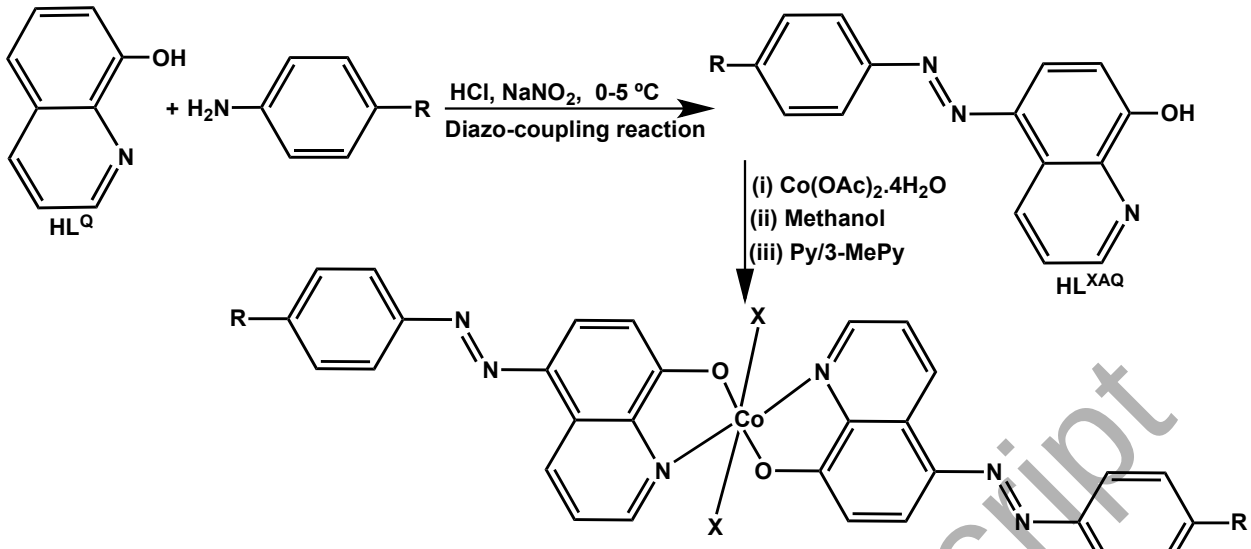

Chemical structures of six coordinate complexes 1-8 where the Co atom is bonded with a secondary ligand X.

R	Abbreviation	X	Complex[a]	Complex No.
H	HL^{PAQ}	Pyridine (Py)	$[Co(L^{PAQ})_2(Py)_2]$	1
		3-Methylpyridine (3-MePy)	$[Co(L^{PAQ})_2(3\text{-}MePy)_2]$	2
Me	HL^{MeAQ}	Pyridine (Py)	$[Co(L^{MeAQ})_2(Py)_2]$	3
OMe	HL^{OMeAQ}	Pyridine (Py)	$[Co(L^{OMeAQ})_2(Py)_2]$	4
OEt	HL^{OEtAQ}	Pyridine (Py)	$[Co(L^{OEtAQ})_2(Py)_2]\cdot S$	5
Cl	HL^{CAQ}	Pyridine (Py)	$[Co(L^{CAQ})_2(Py)_2]$	6
Br	HL^{BAQ}	Pyridine (Py)	$[Co(L^{BAQ})_2(Py)_2]$	7
		3-Methylpyridine (3-MePy)	$[Co(L^{BAQ})_2(3\text{-}MePy)]$	8a
		3-Methylpyridine (3-MePy)	$[Co(L^{BAQ})_2(3\text{-}MePy)]\cdot S$	8b

[a] S refers to solvated molecule(s): S = $2H_2O$ for 5 and S = 2(3-MePy) for 8b

Scheme 1. Synthesis of pro-ligand HL^{XAQ} and schematic representation of the resulting cobalt(II) compounds **1**-**8**.

2. Experimental

2.1. *Materials*

$Co(OAc)_2{\cdot}4H_2O$ (Merck), 8-hydroxyquinoline (Loba Chemie), *p*-ethoxyaniline, *p*-chloroaniline, *p*-bromoaniline (Himedia), pyridine (Merck) and 3-methylpyridine (Spectrochem) were used without further purification. *p*-Toluidine (Merck) and *p*-anisidine (CDH) were purified by crystallization and aniline (Sd fine) was distilled prior to use. The solvents used in the reactions were of AR grade and dried using standard procedures.

2.2. *Physical measurements*

Melting points were measured using a Büchi melting point apparatus (M-560) and are uncorrected. Carbon, hydrogen and nitrogen analyses were performed with a Perkin-Elmer 2400 series II instrument. IR spectra from 4000-400 cm^{-1} were obtained on a Perkin Elmer Spectrum BX series FT-IR spectrophotometer in KBr discs. Absorption measurements were carried out on a Perkin-Elmer Lambda25 spectrophotometer at ambient temperature in freshly prepared DMSO solutions. The electrochemical experiments were performed on an EG&G PAR 273A potentiostat/galvanostat connected to a personal computer through a GPIB interface and by using a three-electrode cell. Cyclic voltammetry was performed in 0.2 M $[NBu_4][BF_4]$ / DMSO solutions at ambient temperature using a platinum disc-working electrode (0.5 mm diameter). The potential was controlled *vs*. a Luggin capillary connected to a silver wire pseudo reference electrode and a platinum auxiliary electrode was employed. The redox potential values of the complexes are quoted relative to SCE; they were measured using cyclic voltammetry in the presence of ferrocene as the internal standard ($E_{1/2}^{ox}$ = 0.44 V *vs*. SCE in DMSO). The $E_{1/2}^{ox}$ redox potential value for ferrocene was measured at 200 $mV \cdot s^{-1}$ in $[^nBu_4N][BF_4]$ / 0.1 M DMSO solution and using the saturated calomel electrode (SCE) as reference. Magnetic measurements were performed by solution ^1H NMR using the Evans' method [30] on a Bruker Avance 400 spectrometer operating at 400.13 MHz for **1-6** and on a Bruker Avance 300 spectrometer operating at 300.13 MHz for **7** and **8** at room temperature in an open-air system. The measurements were performed in a standard 5 mm NMR tube containing the paramagnetic sample dissolved in DMSO-d_6, against a co-axial reference tube filled with the same solvent. The data treatment of NMR signals were done using the MestReNova 9.0.1 program.

2.3. *Synthesis of pro-ligands and cobalt(II) complexes*

The pro-ligands 5-[(*E*)-2-(aryl)-1-diazenyl]quinolin-8-ol (HL^{XAQ}) *viz*., 5-[(*E*)-2-(phenyl)-1-diazenyl]quinolin-8-ol (HL^{PAQ}), 5-[(*E*)-2-(4-methylphenyl)-1-diazenyl]quinolin-8-ol (HL^{MeAQ}), 5-[(*E*)-2-(4-ethoxyphenyl)-1-diazenyl]quinolin-8-ol (HL^{OEtAQ}) and 5-[(*E*)-2-(4-bromophenyl)-1-diazenyl]quinolin-8-ol (HL^{BAQ}) [20e] and 5-[(*E*)-2-(4-methoxyphenyl)-1-diazenyl]quinolin-8-ol (HL^{OMeAQ}) and 5-[(*E*)-2-(4-chlorophenyl)-1-diazenyl]quinolin-8-ol (HL^{CAQ}) [20d], were prepared starting from 8-hydroxyquinoline and the corresponding aniline using conventional diazonium salt chemistry, in accord with literature procedures. In view of the similar preparation

methods employed for **1-8**, only that for $[Co(L^{PAQ})_2(Py)_2]$ (**1**) is described below, as a representative example.

2.3.1. Synthesis of *trans*-bis{5-[(*E*)-2-(phenyl)-1-diazenyl]quinolin-8-olato-k^2*N,O*}-bis(pyridine-k*N*) cobalt(II) (1). $Co(OAc)_2 \cdot 4H_2O$ (0.249 g, 0.999 mmol) in methanol (10 mL) was added dropwise to a stirred solution of HL^{PAQ} (0.5 g, 2.005 mmol) in benzene (50 mL) at room temperature, which resulted in the immediate formation of an orange precipitate. The reaction mixture was heated to reflux for 3 h and then filtered while hot. The residue was washed with hot methanol (3 × 5 mL) to remove undesired materials and dried *in vacuo*. The dried solid was dissolved by heating the benzene solution (5 mL) containing pyridine (0.8 mL, 10.113 mmol) and filtered while hot. Upon cooling to room temperature, the filtrate afforded red-brown crystals of **1**. Yield: 0.44 g (61%). M.p. >300 °C. *Anal*. Found: C, 67.93; H, 4.72; N, 15.90%. Calc. for $C_{40}H_{30}CoN_8O_2$: C, 67.30; H, 4.24; N, 15.71. IR (cm^{-1}): 1596m, 1573m, 1559m, 1499s, 1464s, 1400m, 1322s, 1248s, 1188m, 1171m, 764w, 688w, 464w. Electronic absorption data (DMSO) λ_{max}, nm; (ε [M^{-1} cm^{-1}]): 432 (sh), 490 (13171).

2.3.2. Synthesis of *trans*-bis{5-[(*E*)-2-(phenyl)-1-diazenyl]quinolin-8-olato-k^2*N,O*}-bis(3-methylpyridine-k*N*) cobalt(II) (2). $Co(OAc)_2 \cdot 4H_2O$ (0.249 g, 0.999 mmol) and HL^{PAQ} (0.5 g, 2.005 mmol) were used in the reaction. The dried solid was dissolved by heating the benzene solution (5 mL) containing 3-methylpyridine (1 mL, 10.737 mmol) and filtered while hot. The filtrate upon slow evaporation yielded red brown crystals. Yield: 0.44 g (59%). M.p. >300 °C. *Anal*. Found: C, 67.92; H, 4.75; N, 13.98%. Calc. for $C_{42}H_{34}CoN_8O_2$: C, 68.00; H, 4.62; N, 15.11. IR (cm^{-1}): 1595m, 1567m, 1552m, 1497s, 1462s, 1400m, 1391m, 1325s, 1247s, 1191m, 1171m, 1135m, 1097w, 840m, 791m, 702w, 465w. Electronic absorption data (DMSO) λ_{max}, nm; (ε [M^{-1} cm^{-1}]): 434 (sh), 492 (11570).

2.3.3. Synthesis of *trans*-bis{5-[(*E*)-2-(4-methylphenyl)-1-diazenyl]quinolin-8-olato-k^2*N,O*}-bis(pyridine-k*N*) cobalt(II) (3). $Co(OAc)_2 \cdot 4H_2O$ (0.237 g, 0.951 mmol) and HL^{MeAQ} (0.5 g, 1.899 mmol) were used in the reaction. The dried solid was dissolved in hot chloroform (15 mL) containing pyridine (0.8 ml, 10.113 mmol) followed by dilution with benzene (1 mL) and filtered. The filtrate upon slow evaporation yielded red-brown crystals. Yield: 0.45 g (63%).

M.p. >300 °C. *Anal.* Found: C, 68.32; H, 4.93; N, 15.18%. Calc. for $C_{42}H_{34}CoN_8O_2$: C, 68.00; H, 4.62; N, 15.11. IR (cm^{-1}): 1596m, 1572m, 1552m, 1497s, 1461s, 1393m, 1325s, 1246s, 1188m, 1124m, 1098m, 817w, 793w, 760w, 615w, 463w. Electronic absorption data (DMSO) λ_{max}, nm; (ε [M^{-1} cm^{-1}]): 435 (sh), 486 (11273).

2.3.4. Synthesis of *trans*-bis{5-[(*E*)-2-(4-methoxyphenyl)-1-diazenyl]quinolin-8-olato-k^2*N,O*}-bis(pyridine-k*N*) cobalt(II) (4). $Co(OAc)_2 \cdot 4H_2O$ (0.223 g, 0.895 mmol) and HL^{OMeAQ} (0.5 g, 1.790 mmol) were used in the reaction. The dried solid was dissolved in hot benzene (5 mL) containing pyridine (0.8 mL, 10.113 mmol) and filtered while hot to remove any suspended particles. The filtrate upon slow evaporation afforded red-brown crystals of **4**. Yield: 0.44 g (63%). M.p. >300 °C. *Anal.* Found: C, 65.68; H, 4.40; N, 14.60%. Calc. for $C_{42}H_{34}CoN_8O_4$: C, 65.18; H, 4.43; N, 14.49. IR (cm^{-1}): 1596m, 1579s, 1497s, 1462s, 1402m, 1316s, 1246s, 1191m, 1104m, 1026w, 836m, 819, 760m, 603m, 515w, 470w. Electronic absorption data (DMSO) λ_{max}, nm; (ε [M^{-1} cm^{-1}]): 433 (sh), 498 (12406).

2.3.5. Synthesis of *trans*-bis{5-[(*E*)-2-(4-ethoxyphenyl)-1-diazenyl]quinolin-8-olato-k^2*N,O*}-bis(pyridine-k*N*) cobalt(II) dihydrate (5). $Co(OAc)_2 \cdot 4H_2O$ (0.212 g, 0.851 mmol) and HL^{OEtAQ} (0.5 g, 1.704 mmol) were used in the reaction. The dried solid was dissolved in hot benzene (5 mL) containing pyridine (0.8 ml, 10.113 mmol) and filtered while hot. The filtrate upon slow evaporation afforded red-brown crystals. Yield: 0.46 g (67%). M.p. >300 °C. *Anal.* Found: C, 63.46; H, 5.18; N, 13.03%. Calc. for $C_{44}H_{42}CoN_8O_6$: C, 63.06; H, 5.06; N, 13.38. IR (cm^{-1}): 1597m, 1574m, 1563m, 1497s, 1463s, 1400m, 1320s, 1239s, 1150m, 1093w, 1037w, 836w, 766w, 700w, 474w. Electronic absorption data (DMSO) λ_{max}, nm; (ε [M^{-1} cm^{-1}]): 433 (sh), 498 (12508).

2.3.6. Synthesis of *trans*-bis{5-[(*E*)-2-(4-chlorophenyl)-1-diazenyl]quinolin-8-olato-k^2*N,O*}-bis(pyridine-k*N*) cobalt(II) (6). $Co(OAc)_2 \cdot 4H_2O$ (0.219 g, 0.879 mmol) and HL^{CAQ} (0.5 g, 1.762 mmol) were used in the reaction. The dried solid was dissolved in hot chloroform (15 mL) containing pyridine (0.8 ml, 10.113 mmol) and filtered while hot. The filtrate was diluted with benzene (1 mL) and upon slow evaporation afforded red-brown crystals. Yield: 0.45 g (65%). M.p. >300 °C. *Anal.* Found: C, 61.78; H, 3.26; N, 14.04%. Calc. for $C_{40}H_{28}Cl_2CoN_8O_2$: C, 61.38;

H, 3.61; N, 14.32. IR (cm^{-1}): 1583s, 1561w, 1498s, 1461s, 1429w, 1395m, 1317s, 1245s, 1189m, 1136m, 1107m, 834m, 753m, 603m, 516w, 501w. Electronic absorption data (DMSO) λ_{max}, nm; (ε [M^{-1} cm^{-1}]): 438 (sh), 503 (12343).

2.3.7. Synthesis of *trans*-bis{5-[(*E*)-2-(4-bromoophenyl)-1-diazenyl]quinolin-8-olato-k^2*N,O*}-bis(pyridine-k*N*) cobalt(II) (7). $Co(OAc)_2 \cdot 4H_2O$ (0.190 g, 0.762 mmol) and HL^{BAQ} (0.5 g, 1.523 mmol) were used in the reaction. The dried solid was dissolved in hot chloroform (15 mL) containing pyridine (0.8 mL, 10.113 mmol) and filtered to remove any suspended particles. The filtrate was diluted with benzene (1 mL) and upon slow evaporation afforded red-brown crystals of the desired product. Yield: 0.47 g (70%). M.p. >300 °C. *Anal.* Found: C, 55.35; H, 3.60; N, 12.50%. Calc. for $C_{40}H_{28}Br_2CoN_8O_2$: C, 55.11; H, 3.24; N, 12.86. IR (cm^{-1}): 1596m, 1571m, 1551m, 1499s, 1476m, 1462s, 1421m, 1405s, 1382m, 1323s, 1298m, 1247s, 1187m, 1130m, 829w, 792w, 735w, 702m, 656w, 603m, 466w. Electronic absorption data (DMSO) λ_{max}, nm; (ε [M^{-1} cm^{-1}]): 444 (sh), 508 (10599).

2.3.8. Synthesis of *cis*-bis{5-[(*E*)-2-(4-bromoophenyl)-1-diazenyl]quinolin-8-olato-k^2*N,O*}-bis(3-methylpyridine-k*N*) cobalt(II) (8a) and *trans*-bis{5-[(*E*)-2-(4-bromoophenyl)-1-diazenyl]quinolin-8-olato-k^2*N,O*}-bis(3-methylpyridine-k*N*) cobalt(II) di-(3-methylpyridine) solvate (8b). $Co(OAc)_2 \cdot 4H_2O$ (0.190 g, 0.762 mmol) and HL^{BAQ} (0.5 g, 1.523 mmol) were used in the reaction. The dried solid was dissolved in hot benzene (5 mL) containing 3-methylpyridine (1 ml, 10.737 mmol) and filtered while hot to remove any suspended particles. The filtrate, upon slow evaporation, afforded red-brown, block-shaped and red plate-type crystals as identified after visual inspection using a microscope. Crystals of both morphologies were analyzed by single crystal X-ray crystallography and their identities were confirmed as **8a** and **8b** (refer to the structural discussion). Microanalytical results of the bulk sample containing **8a** and **8b** reflected variable results, which indicated the heterogeneous distributions of the compounds in the bulk sample. The MW of the compounds is the same; methylpyridine molecules of crystallization interfered. Yield of the bulk sample: 0.47 g (68%), M.p. >300 °C and IR (cm^{-1}): 1582s, 1498s, 1462s, 1429m, 1390m, 1317s, 1245s, 1187s, 1137w, 1106w, 1066w, 832w, 781w, 752w, 516w, 500w.

2.4. ***Single-crystal X-ray crystallography***

Crystals of cobalt(II) compounds, **1** (pyridine/benzene), **2** (3-methylpyridine/benzene), **3** (pyridine/benzene/chloroform), **4** (pyridine/benzene), **5** (pyridine/benzene), **6** (pyridine/benzene/chloroform), **7** (pyridine/benzene/chloroform) and **8a** and **8b** (3-methylpyridine/benzene) suitable for single-crystal X-ray structure determination were obtained by slow evaporation of solutions of the respective compounds. The measurements were performed on an Agilent Technologies four circle Gemini (Model No. XD-91-00-000) using Mo Kα radiation (λ = 0.71073 Å) from a fine-focus X-ray source. Data were collected at room temperature using omega scans of 0.5º per frame, and a full sphere of data was obtained. The unit cell parameters and the data reduction were obtained with the CrysAlisPro 1.171.38.41 software from Rigaku Oxford Diffraction [31]. Crystal data and refinement details are collected in table 1, and a comparison of selected bond distances and angles is given in table 2. A representation of all the structures is shown in figure 1 and relevant intermolecular non-covalent interactions in figures 2 and 3. The structures were solved by direct methods using SIR-97 [32] or SHELXS package [33] and refined with SHELXL–2014 [34]. The hydrogen atoms attached to carbon atoms were inserted in geometrically calculated positions and included in the refinement using the riding-model approximation, with the *U*iso(H) defined as 1.2*U*eq of the parent carbon atoms for phenyl and 1.5*U*eq of the parent carbon atoms for the methyl groups. The positions of hydrogen atoms of the crystallization water molecule in **5** were calculated by means of the CALC-OH routine of WinGX System–Version 2014.1 [35]. The structures of **1** and **3-7** contain a disordered benzene (or pyridine) molecule with the ring sitting on an inversion center, which could not be modeled. After running Platon/Squeeze program [36], a total of 43-49 electrons worth of scattering were found in volumes of 143-174 $Å^3$, which fit well for the indicated small molecule(s). In view of the difficulty to identify the disordered molecule unambiguously, it was excluded in the final refinement. For **2**, the quality of the data is low due to very weak diffraction of the crystal. Several attempts to get better crystals failed, but the solved structure is not in doubt, consistent with the related compounds as well as with other characterization results. The residual electron density in **2** is close to a phenyl ring and has no chemical meaning. In addition, for **2** a void volume of 166 $Å^3$ contains 12 electrons and the use of Platon/Squeeze program was not a solution. Least-squares refinements with anisotropic thermal motion parameters for all the

non-hydrogen atoms and isotropic for the remaining atoms were employed. Figures 1-3 were drawn with Mercury CSD (Cambridge structural database) 3.5.1 [36].

3. Results and discussion

3.1. *Synthesis and spectroscopic characterization*

The pro-ligands 5-[(4-(R)-phenyl)-1-diazenyl]quinolin-8-ol (HL^{XAQ}) in benzene upon treatment with a solution of $Co(OAc)_2 \cdot 4H_2O$ in methanol (1:2 molar ratio) afforded the respective Co(II) compounds. In all cases, the immediate formation of a precipitate was noticed. Characterization of the amorphous precipitates revealed compounds of composition $[Co(L^{XAQ})_2]$. They were insoluble in most common organic solvents such as methanol, ethanol, benzene, toluene, chloroform, carbon tetrachloride and dichloromethane even after prolonged heating. These precipitates were soluble in hot DMSO, pyridine and pyridine derivatives such as methylpyridines. Crystallization experiments with $[Co(L^{XAQ})_2]$ using pure DMSO or a combination with other common solvents invariably afforded amorphous materials. However, when a large excess of pyridine (Py) or 3-methylpyridine (3-MePy) was added to a suspension of the $[Co(L^{XAQ})_2]$ compounds in benzene or benzene/chloroform solvent mixture, the isolation of crystalline Co(II) compounds, in which either Py (**1**, **3**-**7**) or 3-MePy (**2**, **8a** and **8b**) was coordinated to the cobalt atoms, became possible. It should be mentioned that crystallization trials for **8** in a solvent mixture of benzene/3-methylpyridine afforded red-brown, block-shaped (**8a**) and red plate-type (**8b**) crystals; both were characterized by single crystal X-ray crystallography. Compounds **5** and **8b** crystallized as solvates with two molecules of H_2O (**5**) or of 3-MePy (**8b**), see scheme 1. The presence of water in **5** is attributed to traces of water present in the solvents and reagents used for the crystallization experiments. The formulations of cobalt compounds **1**-**8** were ascertained from elemental analyses and subsequently by determining their crystal structures. The characteristic IR and electronic absorption data are given in the Experimental section.

3.2. *Description of the X-ray crystal structures*

The asymmetric units of **1**-**7**, **8a** and **8b** comprise half of the compounds molecules, *viz.* a Co(II) cation, one O,N-chelating L^{XAQ} ligand and a N-bound pyridine (**1**, **3**-**7**) or 3-methylpyridine moiety (**2**, **8a** and **8b**), apart from a (disordered) benzene/pyridine (**1**, **3**-**7**) or a 3-methylpyridine

(**8b**) crystallization molecules. The cobalt ions sit on inversion centers, except for **8a** where it stands on a 2-fold axis; upon symmetry expansion, octahedral type complexes with *trans* geometry, excluding **8a**, which has a *cis* configuration, are generated. The *cis* arrangement of the L^{BAQ} ligands in **8a** leads to a distortion of the octahedron around the cobalt cation, as evidenced by (see table 2) O-Co-N (metallacycle) and O-Co-N_L angles of 78.85(10)° and 96.21(11)°, respectively, which are the smallest of all structures, as well as by the O-Co-O angle of 173.56(15)° itself considerably away from the 180° measured for the other compounds. The Co-N_{pyr} distances [2.2047(15) – 2.171(3) Å] are larger than the Co–N_L [2.097(4) – 2.1523(3) Å], probably as a result of charge effects; in **8a** the difference in those two parameters is as small as 0.019 Å (table 2). The N=N bond lengths are in the 1.243(6) – 1.264(4) Å range, typical of double bonds between those atoms when connected to an aromatic ring (table 2) [37].

The L^{XAQ} ligands are almost planar in **1**, **3**, **4**, **6** and **7** as confirmed by the angles of 4.42 – 5.75° between the least-square planes of the quinolone and the phenyl rings (table 2). In **2** and in **8b** this factor assumes values of 27.98° and 23.04°, in this order, probably associated with stereochemical effects arising from the 3-methylpyridine. In **8a** and in **5** the distortions of L^{XAQ} are intermediate, thus evidencing the effect of the geometry of the compound (in the former) and of a bulkier substituent (OEt in the latter). The complexes with evident twisting in L^{XAQ} ligands (**2**, **5**, **8a** and **8b**) are those with longer Co···Co intermolecular distances (table 2).

A search on the Cambridge Structural Database (CSD) [38] was performed to account for the type and variety of metal complexes with 5-substituted (here onward referred to as X) oxyquinolin-8-olate ligands. Forty-six entries pertain to transition metals complexes where, most commonly, X = Cl, Br or NO_2 [39], rarely with X = SO_3 [40], NH_2 [41], or SMe [42]. Taking the related Co(II) complex molecules [39] for comparison, it is worth noting that the Co-O and the Co-N_L distances on the L^{OQ} substituent (in the ranges 1.902-1.917 and 1.878-1.935 Å, respectively), as well as the Co-N_{pyr} bond lengths (1.926-1.982 Å) are considerably shorter than those measured in this work (see table 2), therefore revealing the influence of the unsaturated X-substituent in the oxyquinolin-8-olate ligands on the structural properties of the complexes. In addition, the search also revealed that compounds where X is an unsaturated group are mainly of lanthanides [43] or of yttrium [43a, 44], multinuclear and with the oxyquinolinolate moiety O-bridging metal cations. Rare examples include a discrete copper complex [45] and a polymeric zinc species [46]. Complexes of the main group metals and with 5-X-oxyquinolin-8-olate ligands

specifically with unsaturated X groups include diorganotin(IV) moieties [20b-d]. Discrete aluminum complex molecules with X = SO_2NRR' [47] and sodium dimers with X = Cl [48] are also known.

Strong π···π interactions are found between the substituted phenyl rings of neighboring molecules of **5** with *centroid* distances between the two π-systems of *ca*. 3.82 Å (figure 2(A)). The molecules of **3**, **4**, **6** and **7** are gathered by means of strong intermolecular C–H···π edge-to-face (T-shaped) arrangements [*d*(H···*centroid*) ≤ 2.8 Å; ∠C–H···*centroid* ≤ 177°] (figure 2(B), exemplified for **7**) with the donor pyridine ligand of one molecule almost perpendicular to the acceptor phenyl ring of an adjacent one. In **4**, in addition (figure 2(C)), the pyridine moieties also act as acceptors of one of the methoxy H-atoms of an adjacent molecule [*d*(H···*centroid*) of 2.593 Å; ∠C–H···*centroid* of 153°].

The C–H···π interactions in **2** are different and involve the quinoline moieties (figure 3(A)) which act as acceptors from both an aromatic and a methyl H-atom from 3-methylpyridine of a vicinal molecule [*d*(H···*centroid*) of 2.73 Å, ∠C–H···*centroid* of 176°; *d*(H···*centroid*) of 2.96 Å, ∠C–H···*centroid* of 147°]. In the molecules of **8a** and **8b**, the relevant C–H···π contacts comprise the N-containing ring of a quinoline moiety as acceptor, but the role of donor groups is played by an aromatic H-atom from a coordinated (**8a**) and non-coordinated (**8b**) 3-methylpyridine [in the same order: *d*(H···*centroid*) of 2.81 Å, ∠C–H···*centroid* of 171°; *d*(H···*centroid*) of 2.60 Å, ∠C–H···*centroid* of 161°] (figures 3(B) and 3(C)).

3.3. *Electrochemical properties*

The redox properties of cobalt compounds **1**-**8** (table 3) were studied by cyclic voltammetry at a Pt electrode, in 0.2 M [$^nBu_4N$][BF_4] / DMSO solutions and reveal metal and ligand based redox processes. All the complexes exhibit (see figure 4 for **2** and figure S1 in Supplementary Material file for the remaining compounds) two successive anodic irreversible waves, I^{ox} and II^{ox}, at potential ranges of 0.44 – 0.54 and 0.73 – 0.82 V *vs*. SCE, respectively. The former wave can be tentatively assigned to the Co(II) → Co(III) process and the latter to ligand based oxidation. An intense, broad and irreversible cathodic wave (I^{red}) was also detected between –1.50 V and –1.71 V *vs*. SCE which is believed to involve the Co(II) → Co(I) conversion. The cyclic

voltammetry of **8** did not allow us to distinguish between the *cis* and *trans* isomers in solution, leading us to consider either an interconversion of the compounds in the electrolyte medium, or of a negligible difference on redox potential values. The oxidation potentials of the compounds are close to those found for tryptamine-derived salicylaldimine cobalt(II) compounds [49] and for the di-scorpionate compound $[Co\{HOCH_2C(pz)_3\}_2](NO_3)_2$ [50], but considerably lower than those of the mono-scorpionates $[Co(OSO_3H)(OMe)(HOMe)\{HC(pz)_3\}]$ and $[CoCl_2(H_2O)\{CH_3SO_2OCH_2C(pz)_3\}]$ [51], the dinuclear $[CoCl(\mu\text{-}Cl)(Hpz^{Ph})_3]_2$ or the mononuclear $[CoCl_2(Hpz^{Ph})_4]$ (Hpz^{Ph} = 3-phenylpyrazole).

3.4. *Magnetic studies*

No signals were observed in the ^1H NMR spectra of **1**-**8** as anticipated for the paramagnetic character of the Co(II). The effective magnetic moment (μ_{eff}) of cobalt(II) compounds **1**-**8** was estimated by NMR using Evans' method [30]. This method relates the difference in the chemical shift of an inert reference compound in the presence and in the absence of a paramagnetic species. In the present work, equation A was applied where χ_m^P is the mass susceptibility, Δf is the observed difference in frequency, f is the spectrometer frequency, m is the concentration of the paramagnetic substance, χ_0 is the mass susceptibility of the solvent, and d_0 and d_s are the densities of the solvent and of the solution, respectively.

$$\chi_m^P = \frac{3\Delta f}{4\pi f m} + \chi_0 + \frac{\chi_0(d_0 - d_s)}{m} \qquad \text{(A)}$$

With the obtained mass susceptibility, the molar susceptibility (χ_M^P) was calculated and then applied in expression B (where K_B is the Boltzmann constant, N_A the Avogadro's number, β the Bohr magneton and T the absolute temperature).

$$\mu_{eff} = \sqrt{\frac{3K_B}{N_A\beta^2}(\chi_M^P T)} \qquad \text{(B)}$$

In the present study, a co-axial double NMR tube was used, with DMSO-d_6 both as solvent and as internal standard since the resonance of this species (a quintet at δ 2.50 relative to TMS) was clearly shifted by the additional magnetic field of the Co(II) paramagnetic compounds (figure 5).

The magnetic measurements for **1**-**8** (tables 4 and S1) led to effective magnetic moments between 4.34 and 4.99 B.M., which are in the expected range for cobalt metal ions with octahedral geometry and d^7 high spin (t_{2g}^5 e_g^2) configuration. The exception is **6** (μ_{eff} = 3.67 μ_β) with an intermediate value between the expected ones for high and low-spin configurations [52].

4. Conclusion

A series of new Co(II) compounds **1**-**8** based on HL^{XAQ} have been synthesized. They were characterized by IR and UV-vis spectroscopies and by single-crystal X-ray diffraction analysis. The compounds are all octahedral displaying *trans* geometries except for **8a**, which has a *cis* configuration. The compounds are redox active with Co(II) $\rightarrow$ Co(III) oxidation waves at potentials of 0.44 – 0.54 V *vs*. SCE and Co(II) $\rightarrow$ Co(I) cathodic processes at –1.50 V and –1.71 V *vs*. SCE. The magnetic moments of most of the compounds are in the 4.34 - 4.99 B.M. range that agree with the octahedral geometry and suggest d^7 high spin (t_{2g}^5 e_g^2) configurations.

Supplementary material

CCDC 1835529-1835537 contain the supplementary crystallographic data for **8b**, **8a**, **2**, **1**, **7**, **4**-**6** and **3**, in this order. These data can be obtained free of charge via www.ccdc.cam.ac.uk/getstructures. ESI file contains the cyclic voltammograms of **1**, **3**-**8** (figure S1) and the table with the data and parameters obtained by Evans NMR method (table S1).

Acknowledgements

The financial support of the University Grants Commission, New Delhi (Grant No. 42-396/2013 (SR) 2013, TSBB), the Council of Scientific and Industrial Research, New Delhi (Grant No. 01 (2734)/13/EMR-II, 2013, TSBB) and of the Foundation for Science and Technology (FCT), Portugal (Project UID/QUI/00100/2013, MFCGS and BGMR). KN thanks the University Grants Commission (UGC), New Delhi, for UGC-RGNF research fellowship. Authors (TSBB, KN) acknowledge DST-PURSE for the diffractometer facility.

References

[1] J. Mendham, R.C. Denny, J.D. Barnes, M.J.K. Thomas, *Vogel's Quantitative Chemical Analysis*, Prentice Hall, London (2000).

[2] D.C. Harris, *Quantitative Chemical Analysis*, Freeman, New York (2010).

[3] V. Oliveri, G. Vecchio. *Eur. J. Med. Chem.*, **120**, 252 (2016).

[4] M. Albrecht, M. Fiege, O. Osetska. *Coord. Chem. Rev.*, **252**, 812 (2008).

[5] F. Qian, Y. Li, S. Gradecak, D. Wang, C.J. Barrelet, C.M. Lieber. *Nano Lett.*, **4**, 1975 (2004).

[6] Y.S. Zhao, C. Di, W. Yang, G. Yu, Y. Liu, J. Yao. *Adv. Funct. Mater.*, **16**, 1985 (2006).

[7] C.W. Tang, S.A. Van Slyke. *J. Appl. Phys.*, **65**, 3610 (1989).

[8] R.H. Friend, R.W. Gymer, A.B. Holmes, J.H. Burroughes, R.N. Marks, C. Taliani, D.A. Dos Santos, J.L. Bredas, M. Logdlund, W.R. Salaneck. *Nature*, **397**, 121 (1999).

[9] S.C. Lyu, Y. Zhang, C.J. Lee. *Chem. Mater.*, **15**, 3294 (2003).

[10] S. Meloni, A. Palma, J. Schwartz, A. Kahn, R. Car. *J. Am. Chem. Soc.*, **125**, 7808 (2003).

[11] A. Mishra, P.K. Nayak, N. Periasamy. *Tetrahedron Lett.*, **45**, 6265 (2004).

[12] L.M. Leung, W.Y. Lo, S.K. So, K.M. Lee, W.K. Choi. *J. Am. Chem. Soc.*, **122**, 5640 (2000).

[13] M.E. Mahmoud, S.S. Haggag, T.M. Abdel-Fattah. *Polyhedron*, **28**, 181 (2009).

[14] L. liu, L. Wang, D. Jia. *J. Coord. Chem.*, **61**, 1019 (2008).

[15] P. Khakhlary, C.E. Anson, A. Mondal, A.K. Powell, J.B. Baruah. *Dalton Trans.*, **44**, 2964 (2015).

[16] (a) J. Matheus. *Ber.*, **21**, 1644 (1888). (b) F.J. Welcher, *Organic Analytical Regents*, Vol. 1, Van Nostrand, London (1947). (c) V.M. Ivanov, T.F. Rudometkina. *Zh. Anal. Khim.*, **33**, 2426 (1978).

[17] (a) T.S. Basu Baul, T.K. Chattopadhyay, B. Majee. *Ind. J. Chem., Sect. A*, **23**, 470 (1984). (b) I. Aiello, M. Ghedini, C. Zanchini. *Inorg. Chim. Acta*, **255**, 133 (1997). (c) R. Sarkar, P. Mondal, K.K. Rajak. *Dalton Trans.*, **43**, 2859 (2014). (d) S.A. Abdel-Latif, H. Moustafa. *Appl. Organomet. Chem.*, **31**, e3876 (2017).

[18] E. El-Sawi, F.A. Moti, S. El-Messary. *Bull. Soc. Chim. (Belg.)*, **94**, 69 (1985).

[19] T.S. Basu Baul, D. Dey. *Synth. React. Inorg. Met.-Org. Chem.*, **19**, 101 (1989).

[20] (a) K.D. Ghuge, P. Umapathy, M.P. Gupta, D.N. Sen. *Inorg. Nucl. Chem.*, **43**, 653 (1981). (b) T.S. Basu Baul, T.K. Chattopadhyay, B. Majee. *Polyhedron*, **2**, 635 (1983). (c) B.K. Deb, A.K. Ghosh. *Can. J. Chem.*, **65**, 1241 (1987). (d) T.S. Basu Baul, A. Mizar, X. Song, G. Eng, R. Jirásko, M. Holčapek, R. Willem, M. Biesemans, I. Verbruggen, R. Butcher. *J. Organomet. Chem.*, **691**, 2605 (2006). (e) T.S. Basu Baul, A. Mizar, A. Lyčka, E. Rivarola, R. Jirásko, M. Holčapek, D. de Vos, U. Englert. *J. Organomet. Chem.*, **691**, 3416 (2006). (f) T.S. Basu Baul, A. Mizar, E. Rivarola, U. Englert. *J. Organomet. Chem.*, **693**, 1751 (2008). (g) T.S. Basu Baul, A. Mizar, A.K. Chandra, X. Song, G. Eng, R. Jirásko, Holčapek, D. de Vos, A. Linden. *J. Inorg. Biochem.*, **102**, 1719 (2008). (h) T.S. Basu Baul, A. Mizar, G. Ruisi, E.R.T. Tiekink. *Z. Anorg. Allg. Chem.*, **638**, 664 (2012). (i) T.S. Basu Baul, A. Mizar, G. Eng, R. Far, A. Linden. *J. Coord. Chem.*, **66**, 813 (2013).

[21] T.S. Basu Baul, A. Mizar, A. Paul, G. Ruisi, R. Willem, M. Biesemans, A. Linden. *J. Organomet. Chem.*, **694**, 2142 (2009).

[22] A.Z. El-Sonbati, R.M. Issa, A.M. Abd El-Gawad. *Spectrochim. Acta, Part A*, **68**, 134 (2007).

[23] F.-Y. Wu, X.-F. Tan, Y.-M. Wu, Y.-Q. Zhao. *Spectrochim. Acta, Part A*, **65**, 925 (2006).

[24] (a) M. Hébrant, M. Rose-Hélène, J.-P. Joly, A. Walcarius. *Colloids Surf. A*, **380**, 261 (2011). (b) M. Hébrant, M. Rose-Hélène, A. Walcarius. *Colloids Surf. A*, **417**, 65 (2013).

[25] S.M. Seleim, T.A. Hamdalla, M.E. Mahmoud. *Spectrochim. Acta, Part A*, **184**, 134 (2017).

[26] J.M.D. Coey, *Magnetism and Magnetic Materials*, Cambridge University Press, New York (2010).

[27] C. Sgarlata, V. Oliveri, J. Spencer. *Eur. J. Inorg. Chem.*, **36**, 5886 (2015).

[28] S. Natarajan, G. Shanmugam, S.A. Martin. *Cryst. Res. Technol.*, **43**, 561 (2008).

[29] T.S. Basu Baul, K. Nongsiej, K. Biswas, S.R. Joshi, H. Höpfl, submitted for publication.

[30] (a) D.F. Evans. *J. Chem. Soc*., 2003 (1959). (b) E.M. Schubert. *J. Chem. Educ.*, **69**, 62 (1992).

[31] *CrysAlisPro* 1.171.38.41, Rigaku Oxford Diffraction (2015).

[32] A. Altomare, M.C. Burla, M. Camalli, G.L. Cascarano, C. Giacovazzo, A. Guagliardi, A.G.G. Moliterni, G. Polidori, R. Spagna. *J. Appl. Cryst.*, **32**, 115 (1999).

[33] G.M. Sheldrick. *Acta Crystallogr., Sect. A*, **64**, 112 (2008).

[34] L.J. Farrugia. *J. Appl. Cryst.*, **45**, 849 (2012).

[35] A.L. Spek. *Acta Crystallogr., Sect. C*, **71**, 9 (2015).

[36] C.F. Macrae, I.J. Bruno, J.A. Chisholm, P.R. Edgington, P. McCabe, E. Pidcock, L. Rodriguez-Monge, R. Taylor, J. van de Streek, P.A. Wood. *J. Appl. Cryst.*, **41**, 466 (2008).

[37] F.H. Allen, O. Kennard, D.G. Watson, L. Brammer, A. Guy Orpen. *J. Chem. Soc., Perkin Trans. II*, S1 (1987).

[38] See the Cambridge Structural Data Base, CSD version 1.22, May 2018.

[39] Involving solely cobalt(II) complex molecules, see *e.g.* (a) H.-R. Zhang, T. Meng, Y.-C. Liu, Z.-F. Chen, Y.-N. Liu, H. Liang. *Appl. Organomet. Chem.*, **30**, 740 (2016). (b) H.-R. Zhang, K.-B. Huang, Z.-F. Chen, Y.-C. Liu, Y.-N. Liu, T. Meng, Q.-P. Qin, B.-Q. Zou, H. Liang. *MedChemComm*, **7**, 806 (2016).

[40] (a) F. Camerel, A. Vacher, O. Jeannin, J. Barbera, M. Fourmigue. *Chem. Eur. J.*, **21**, 19149 (2015). (b) W.-L. Zhang, Y.-Y. Liu, J.-F. Ma, H. Jiang, J. Yang, G.-J. Ping. *Cryst. Growth Des.*, **8**, 1250 (2008).

[41] X. Chen, F.J. Femia, J.W. Babich, J. Zubieta. *Inorg. Chim. Acta*, **308**, 80 (2000).

[42] L. Pech, Yu. Bankovsky, I. Berzina, V. Belsky, J. Ashaks. *Latv. Khim. Z.*, No. 3, 19 (1997).

[43] See, *e.g.* (a) H.-L. Gao, L. Jiang, S. Liu, H.-Y. Shen, W.-M. Wang, J.-Z. Cui. *Dalton Trans.*, **45**, 253 (2016). (b) H.-L. Gao, X.-P. Zhou, Y.-X. Bi, H.-Y. Shen, W.-M. Wang, N.-N. Wang, Y.-X. Chang, R.-X. Zhang, J.-Z. Cui. *Dalton Trans.*, **46**, 4669 (2017). (c) Y.-X. Zhang, M. Li, B.-Y. Liu, Z.-L. Wu, H.-Y. Wei, W.-M. Wang. *RSC Adv.*, **7**, 55523 (2017). (d) H.-L. Gao, S.-X. Huang, X.-P. Zhou, Z. Liu, J.-Z. Cui. *Dalton Trans.*, **47**, 3503 (2018). (e) W.-M. Wang, Y.-X. Zhang, J.-C. Zhao, X.-H. Zhang, Y. Tan, Y.-Y. Cui, Y. Shi, Z.-L. Wu. *Polyhedron*, **146**, 161 (2018).

[44] H.-L. Gao, L. Jiang, W.-M. Wang, S.-Y. Wang, H.-X. Zhang, J.-Z. Cui. *Inorg. Chem.*, **55**, 8898 (2016).

[45] Y.-N. Luo, X.-Z. Xu, X. Zhang, X.-Y. Yu, X.-S. Qu. *Wuji Huaxue Xuebao*, **29**, 2655 (2013).

[46] X.-W. Wu, D. Zhang, Z.-H. Wu, J.-P. Ma. *Jiegou Huaxue*, **33**, 1326 (2014).

[47] J.-A. Cheng, H.-P.D. Shieh. *Anal. Sci.: X-Ray Struct. Anal. Online*, **24**, x235 (2008).

[48] A.J. Middleton, W.J. Marshall, N.S. Radu. *J. Am. Chem. Soc.*, **125**, 880 (2003).

[49] Y.-Y. Tong, M.F.C. Guedes da Silva, J.J.R. Fraústo da Silva, A.J.L. Pombeiro, P. Martin-Zarga, G. Martin, P. Gili. *Port. Electrochim. Acta*, **11**, 87 (1993).

[50] T.F.S. Silva, L.M.D.R.S. Martins, M.F.C. Guedes da Silva, A.R. Fernandes, A. Silva, P.M. Borralho, S. Santos, C.M.P. Rodrigues, A.J.L. Pombeiro. *Dalton Trans.*, **41**, 12888 (2012).

[51] T.F.S. Silva, L.M.D.R.S. Martins, M.F.C. Guedes da Silva, M.L. Kuznetsov, A.R. Fernandes, A. Silva, C.-J. Pan, J.-F. Lee, B.J. Hwang, A.J.L. Pombeiro. *Chem.-Asian J.*, **9**, 1132 (2014).

[52] F.A. Cotton, G. Wilkinson, *Advanced Inorganic Chemistry*, 3rd Edn., Wiley, New York (1972), pp. 535-542.

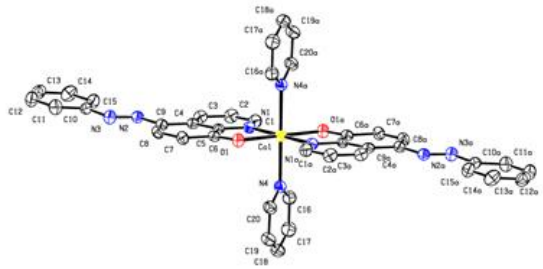

1

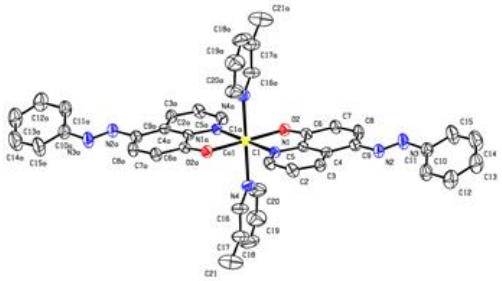

2

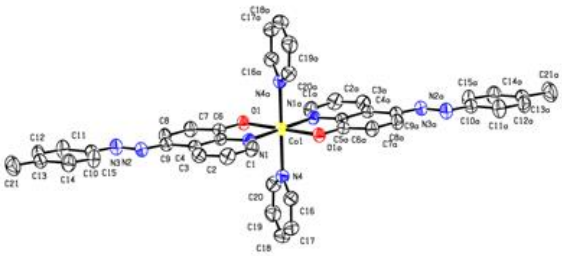

3

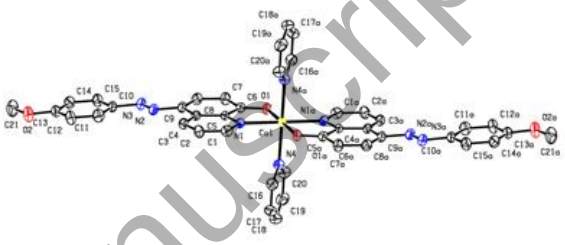

4

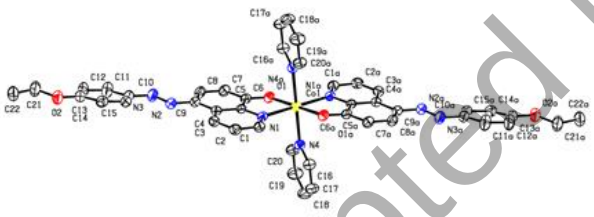

5

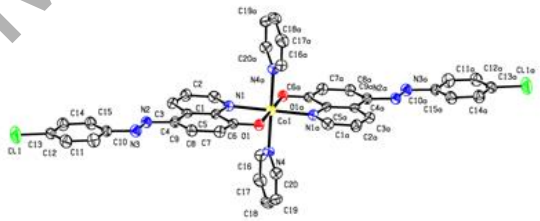

6

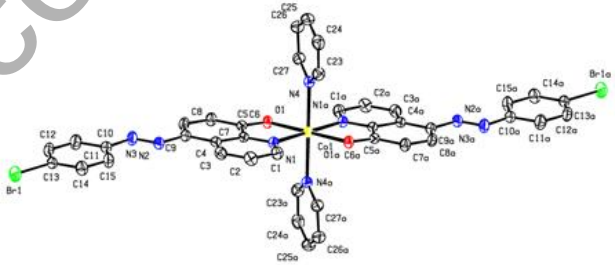

7

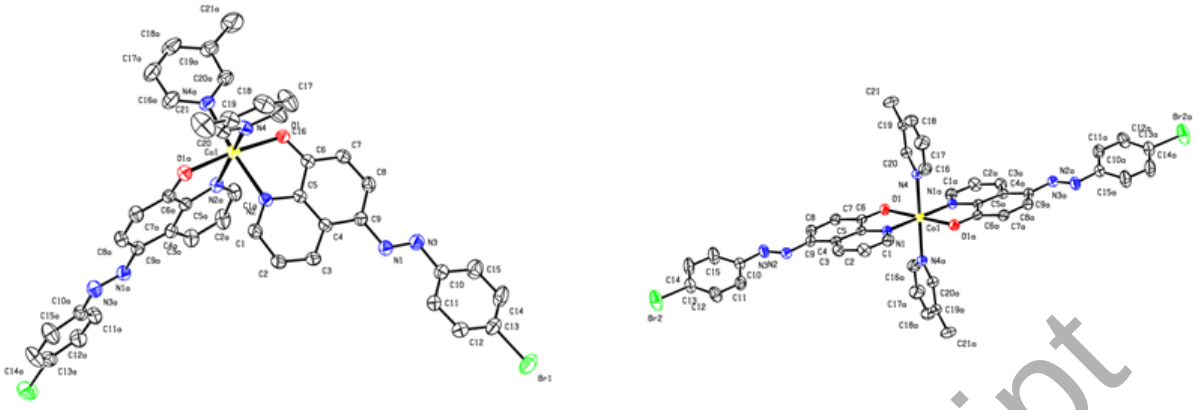

8a **8b**

Figure 1. Perspective views of **1**-**7**, **8a** and **8b** with the atom numbering schemes. Displacement ellipsoids are drawn at the 30% probability level and hydrogens are omitted for clarity. Symmetry operations "*a*" to generate equivalent atoms: -x, 2-y,1-z (**1**); 1-x,1-y,1-z (**2** and **3**); 1-x,1-y,-z (**4** and **8b**); -x,1-y,-z (**5**); -x,-y,2-z (**6**); 2-x,2-y,1-z (**7**); 1-x,y,1/2-z (**8a**). For **5** and **8b**, the non-coordinated water or 3-methylpyridine molecules, respectively, are omitted for clarity.

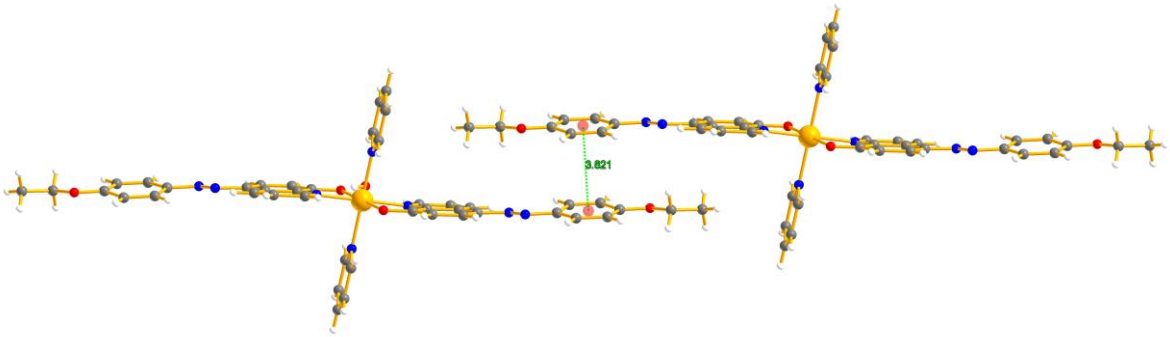

(2A)

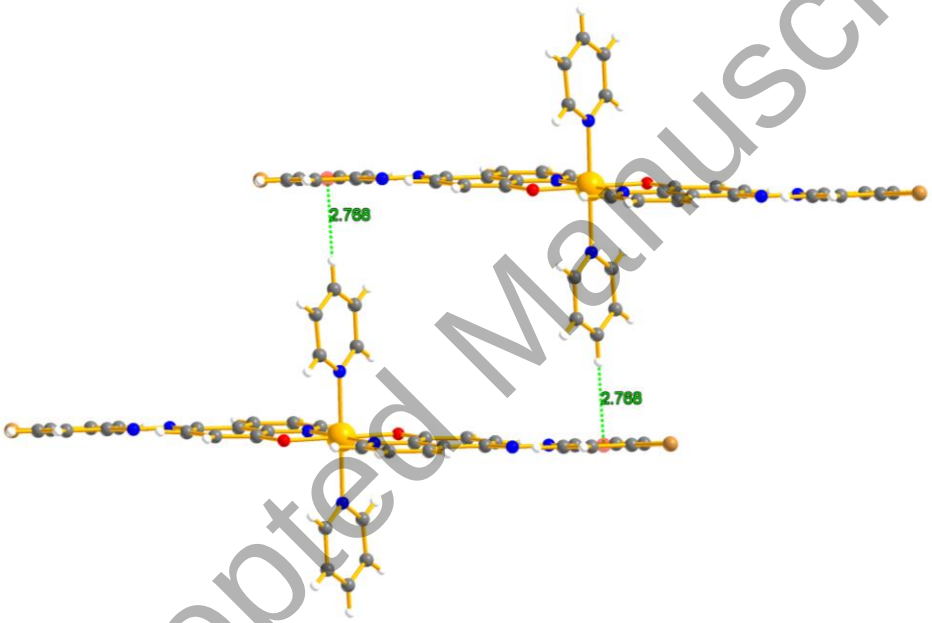

(2B)

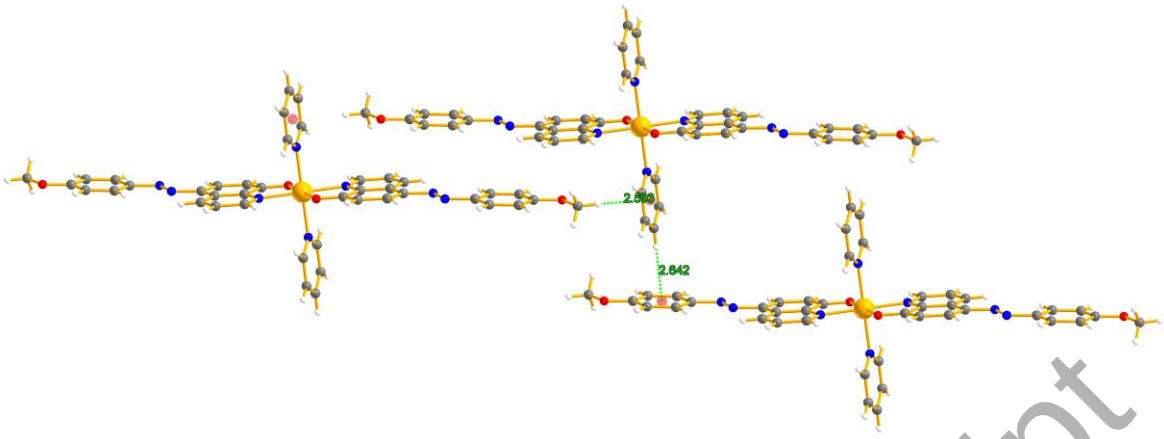

(2C)

Figure 2. (A) π···π interactions found between the molecules of **5**; (B) Intermolecular C–H···π edge-to-face (T-shaped) arrangements in the structure of **7**: *d*(H25···*centroid*) = 2.768 Å, ∠ C25–H25···*centroid* = 178°; (C) Intermolecular C–H···π arrangements in the structure of **4**: *d*(H21B···*centroid*) = 2.593 Å, ∠ C21–H21B···*centroid* = 153°; *d*(H18···*centroid*) = 2.642 Å, ∠ C18–H18···*centroid* = 177°.

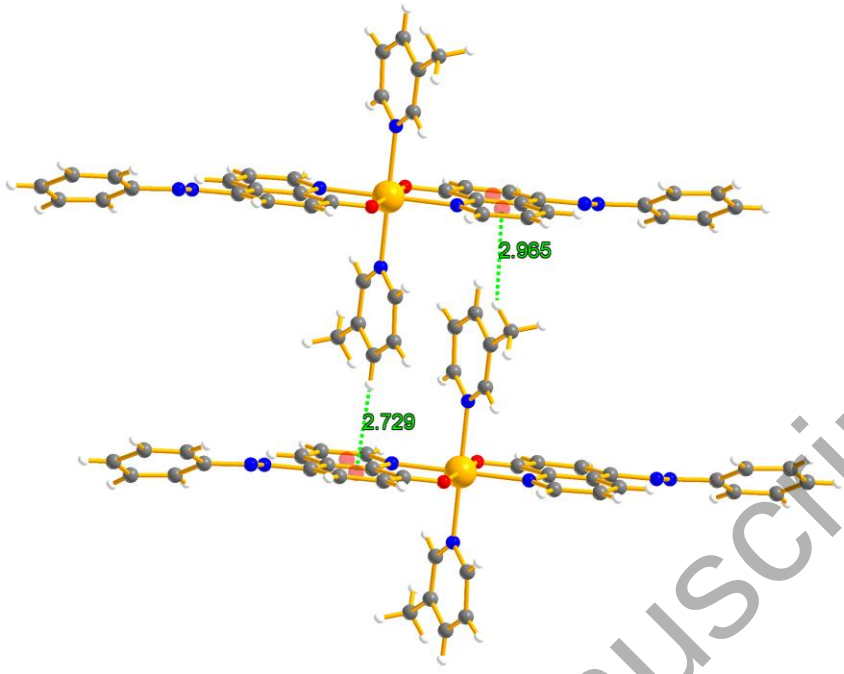

(3A)

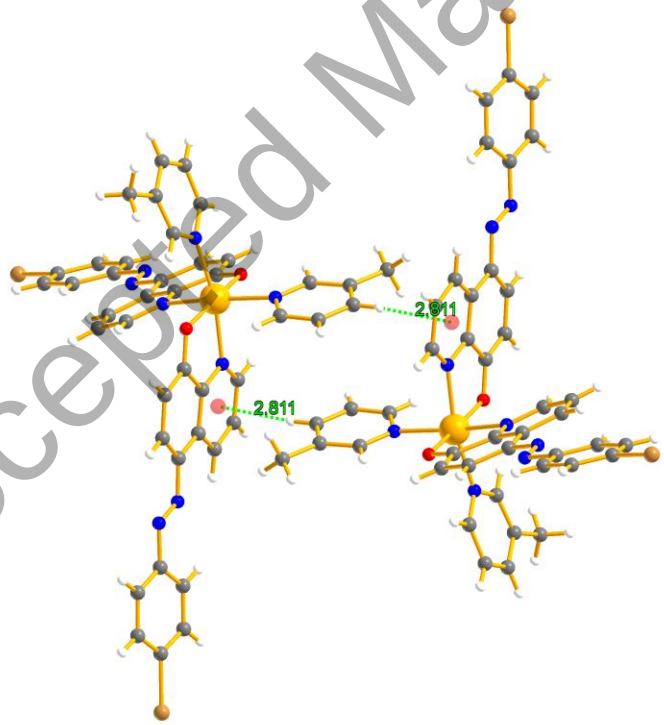

(3B)

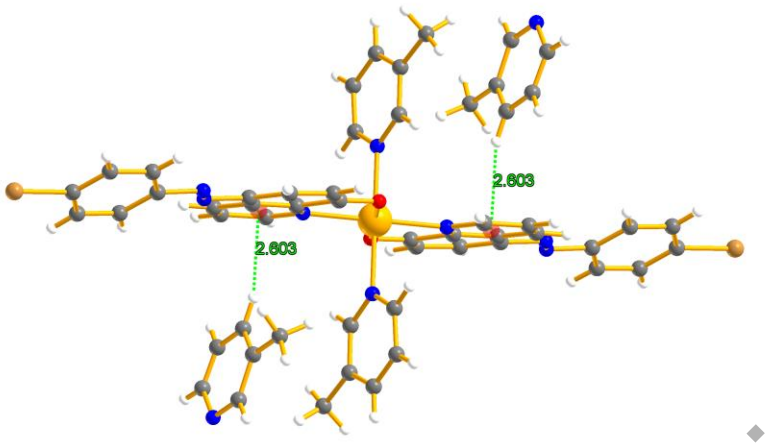

(3C)

Figure 3. (A) Intermolecular C–H···π arrangements in the structure of **2**: *d*(H18···*centroid*) = 2.729 Å, ∠ C18–H18···*centroid* = 176°; *d*(H21A···*centroid*) = 2.965 Å, ∠ C21–H21A···*centroid* = 147°; (B) Intermolecular C–H···π arrangements in the structure of **8a**: *d*(H18···*centroid*) = 2.811 Å, ∠ C18–H18···*centroid* = 171°; (**C**) Intermolecular C–H···π arrangements in the structure of **8b**: *d*(H26···*centroid*) = 2.603 Å, ∠ C26–H26···*centroid* = 161°.

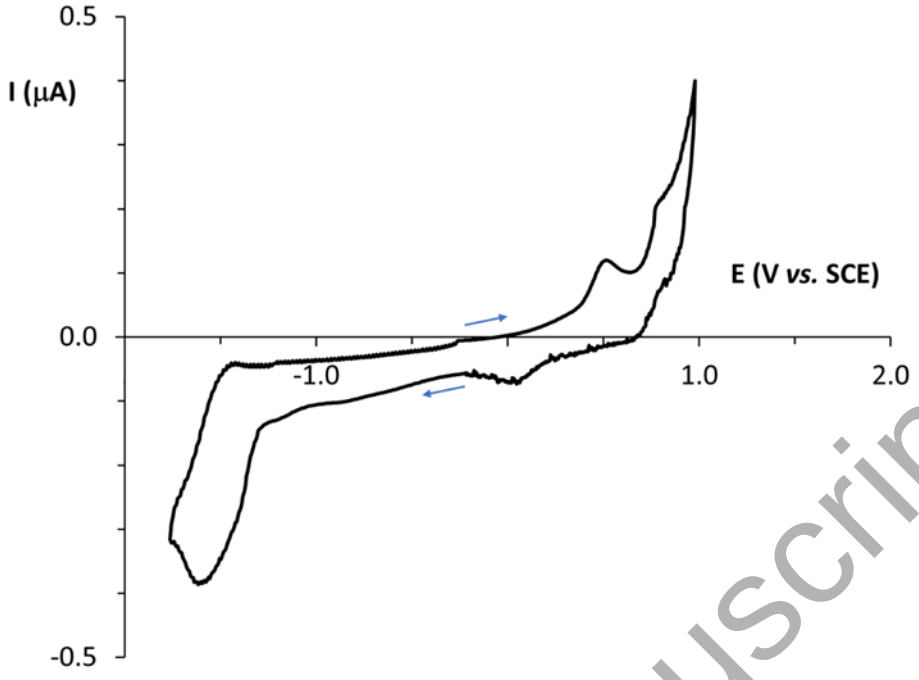

Figure 4. Cyclic voltammogram of **2** (3.7×10^{-3} M) in 0.2 M $[NBu_4][BF_4]$ / DMSO at a platinum disc working electrode (d = 0.5 mm) and at a scan rate of 0.2 $V\cdot s^{-1}$. The arrows indicate the initial (anodic or cathodic) potential scan direction.

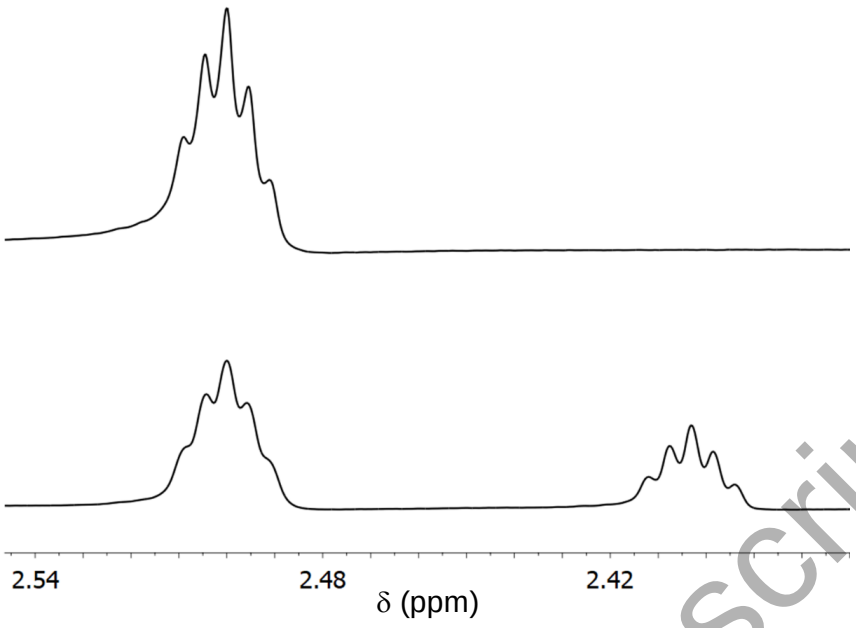

Figure 5. ^{1}H NMR spectrum of DMSO-d_6 in the absence (top) and in the presence (bottom) of **2**.

Table 1. Crystal data, data collection parameters and convergence results for **1**-**8**.

	1	**2**	**3**	**4**	**5**	**6**	**7**	**8a**	**8b**
CCDC No.									
Empirical formula	$C_{40}H_{30}CoN_8O_2$	$C_{42}H_{34}CoN_8O_2$	$C_{42}H_{34}CoN_8O_2$	$C_{42}H_{34}CoN_8O_4$	$C_{44}H_{42}CoN_8O_6$	$C_{40}H_{28}Cl_2CoN_8O_2$	$C_{40}H_{28}Br_2CoN_8O_2$	$C_{42}H_{32}Br_2CoN_8O_2$	$C_{54}H_{46}Br_2CoN_{10}O_2$
Formula weight	713.65	741.70	741.70	773.70	837.78	782.53	871.45	899.50	1083.77
Crystal size (mm)	0.21×0.21×0.23	0.08×0.15×0.10	0.02×0.22×0.30	0.14×0.16×0.16	0.15×0.18×0.35	0.12×0.25×0.29	0.15×0.23×0.29	0.12×0.17×0.26	0.05×0.12×0.16
Crystal shape	Block	Block	Block	Block	Plate	Plate	Block	Block	Plate
Temperature (K)	291(2)	288(2)	290(2)	291(2)	290(2)	292(2)			
Crystal system	Triclinic	Triclinic	Triclinic	Triclinic	Triclinic	Triclinic	Triclinic	Monoclinic	Triclinic
Space group	*P* -1	*P* -1	*P* -1	*P* -1	*P* -1	*P* -1	*P* -1	*C* 2/c	*P* -1
a (Å)	8.6204(4)	9.5194(9)	8.3398(5)	8.3893(15)	9.3275(4)	8.3607(4)	8.3435(5)	21.8738(12)	9.5858(7)
b (Å)	10.4136(6)	10.4999(9)	10.9376(7)	11.1480(17)	10.9526(6)	10.9519(8)	11.0350(8)	10.5034(5)	11.3587(8)
c (Å)	10.8736(6)	11.9273(11)	11.3691(8)	11.2985(17)	13.1207(7)	11.2845(8)	11.3934(8)	17.9354(8)	12.5055(9)
α (º)	93.781(5)	65.975(9)	98.851(5)	100.096(13)	93.722(4)	98.660(6)	99.104(6)	90	106.055(7)
β (º)	92.659(4)	70.919(9)	90.973(5)	93.632(14)	109.194(4)	90.993(5)	91.195(5)	104.997(5)	93.340(6)
γ (º)	92.575(4)	76.455(8)	95.841(5)	93.083(14)	111.930(5)	95.516(5)	95.434(5)	90	107.070(6)
V (Å^3)	971.82(9)	1021.98(18)	1018.83(12)	1036.0(3)	1147.03(11)	1016.23(12)	1030.44(12)	3980.3(4)	1236.38(16)
Z	1	1	1	1	1	1	1	4	1
D_{calc} (g/cm^3)	1.219	1.205	1.209	1.240	1.213	1.279	1.404	1.501	1.458
μ (mm^{-1})	0.485	0.463	0.465	0.463	0.427	0.597	2.398	2.486	2.016
Reflections measured	7662	7096	7532	8089	8330	7974	8057	8658	9143
Independent reflections	4392	4181	4607	4784	5185	4587	4644	4498	5549
Reflection with I > 2σ(I)	3515	2450	3763	2351	3653	2608	3312	2998	3317
Number of parameters	232	242	242	251	275	241	241	250	304
R_{int}	0.0189	0.0505	0.0274	0.0775	0.0248	0.1115	0.0244	0.0263	0.0390
$R(F)$ ($I \geq 2\sigma$)	0.0416	0.1179	0.0446	0.0768	0.0543	0.0713	0.0468	0.0540	0.0642
wR (F^2)	0.1046	0.3624	0.1141	0.2829	0.1466	0.1566	0.1181	0.1507	0.1486

(all data)									
GOF (F^2)	1.031	1.120	1.026	0.760	1.011	0.985	1.040	1.000	1.016
Max., min. Δρ (e/Å^3)	0.293, -0.261	2.242, -0.336	0.327, -0.258	0.355, -0.360	0.269, -0.410	0.443, -0.408	0.740, -0.687	1.082, -0.679	0.560, -0.495

Table 2. Selected bond lengths (Å) and and angles (°) for compounds **1**-**8**.

	1	**2**	**3**	**4**	**5****	**6**	**7**	**8a**	**8b**
N-N	1.256(2)	1.258(9)	1.250(2)	1.243(6)	1.259(3)	1.262(4)	1.253(4)	1.264(4)	1.258(4)
Co-O	2.0517(12)	2.039(5)	2.0421(13)	2.027(4)	2.0303(16)	2.050(2)	2.0560(19)	2.055(2)	2.038(3)
Co-N_L	2.1187(16)	2.108(6)	2.0988(16)	2.097(4)	2.1373(19)	2.103(3)	2.103(2)	2.152(3)	2.121(3)
Co-N_{pyr}	2.2047(15)	2.203(6)	2.2004(16)	2.196(4)	2.199(2)	2.200(3)	2.203(2)	2.171(3)	2.209(3)
O-Co-O	180.00(7)	180.0	180.0	180.0	180.0	180.0	180.00(7)	173.56(15)	180.0
O-Co-N (metallacycle)	80.48(5)	80.5(2)	80.87(5)	80.61(15)	79.96(7)	80.95(11)	80.69(8)	78.85(10)	80.35(11)
O-Co-N	99.52(5)	99.5(2)	99.14(5)	99.39(15)	100.04(7)	99.05(11)	99.31(8)	96.21(11)	99.65(11)
∠ l.s. quinoline-phenyl	5.19	27.98	5.15	4.72	10.26	4.92	5.75	11.13	23.04
∠ l.s. quinoline-pyridine	86.61	85.86	85.09	87.92	79.95	86.30	86.10	87.85	86.61
Co···Co	8.820	9.519	8.340	8.389	9.328	8.361	8.344	9.302	9.586

Graphical abstract